Particle acceleration in magnetically dominated jets

John Kirk Simone Giacchè

Max-Planck-Institut für Kernphysik Heidelberg, Germany

Beyond a PeV, IAP, 16th September 2016

Outline

- Introduction — how to dissipate EM fields
- Under-dense plasmas in jets?
- Two-fluid, test-particle and Monte-Carlo simulations of particle acceleration

Problem

- Relativistic jets are launched with high magnetization parameter: $\sigma \gg 1$.
- Collimation slow $\Rightarrow \sigma \gtrsim 1$, even at pc scale.

  Lyubarsky MN 2010
- *Shocks* (Fermi I acceleration) don't work well for $\sigma \gtrsim 10^{-3}$ (generically perpendicular, low compression).
- *Reconnection* needs a current sheet and a trigger.

Potential Solution

- Embedded fluctuations of the magnetic field (not Lorentz factor) e.g., twists, reversals of polarity at launch.
- Importance increases with radius: $\omega_\mathrm{p} \propto 1/r$.

Potential Solution

- Embedded fluctuations of the magnetic field (not Lorentz factor) e.g., twists, reversals of polarity at launch.
- Importance increases with radius: $\omega_{\rm p} \propto 1/r$.
- Wait long enough JK & Mochol (2011)

Potential Solution

- Embedded fluctuations of the magnetic field (not Lorentz factor) e.g., twists, reversals of polarity at launch.
- Importance increases with radius: $\omega_{\rm p} \propto 1/r$.
- Wait long enough JK & Mochol (2011)
- Hit an obstacle:
  - *MHD*: compress current sheets at a weak shock $\Rightarrow$ enhance reconnection rate.
    Solar wind: Drake et al (2010), relativistic wind: Sironi & Spitkovsky (2011)
  - *Under-dense plasma*: fluctuations reflected as electromagnetic modes forming a dissipative precursor

    Amano & Kirk (2013), Mochol & Kirk (2013)

Under-dense zones in a conical $e^{\pm}$ jet/beam

Three dimensionless jet parameters:

Under-dense zones in a conical $e^{\pm}$ jet/beam

Three dimensionless jet parameters:

1. $(\text{Mass-loading})^{-1}$ $\mu = L/\dot{M}c^2$
2. Magnetization $\sigma_0 = \text{Poynting flux}/\text{K.E. flux}$
3. *A parameter describing the jet composition: e/m*

Under-dense zones in a conical $e^{\pm}$ jet/beam

Three dimensionless jet parameters:

1. $(\text{Mass-loading})^{-1}\ \mu = L/\dot{M}c^2$
2. Magnetization $\sigma_0 = \text{Poynting flux}/\text{K.E. flux}$
3. *A parameter describing the jet composition: e/m*
   - Cross-jet potential $\times\, e/mc^2$: $a_0 = eBr/mc^2$

Under-dense zones in a conical $e^{\pm}$ jet/beam

Three dimensionless jet parameters:

1. $(\text{Mass-loading})^{-1}$ $\mu = L/\dot{M}c^2$
2. Magnetization $\sigma_0 = \text{Poynting flux/K.E. flux}$
3. *A parameter describing the jet composition: e/m*
   - Cross-jet potential $\times\, e/mc^2$: $a_0 = eBr/mc^2$
   - $(\text{Dimensionless luminosity/unit solid angle})^{1/2}$:

     $a_0 = (4\pi L/\Omega_s)^{1/2} \left(e^2/m^2c^5\right)^{1/2}$

Under-dense zones in a conical $e^{\pm}$ jet/beam

Three dimensionless jet parameters:

1. $(\text{Mass-loading})^{-1}$ $\mu = L/\dot{M}c^2$
2. Magnetization $\sigma_0 = \text{Poynting flux}/\text{K.E. flux}$
3. *A parameter describing the jet composition: e/m*
    - Cross-jet potential $\times\, e/mc^2$: $a_0 = eBr/mc^2$
    - (Dimensionless luminosity/unit solid angle)$^{1/2}$:

      $a_0 = (4\pi L/\Omega_s)^{1/2}\left(e^2/m^2c^5\right)^{1/2}$

Constraints/Estimates:

1. $a_0 = 3.4 \times 10^{14}\sqrt{4\pi L_{46}/\Omega_s}$
2. $\sigma_0 \lesssim \mu^{2/3}$ (for a supermagnetosonic jet)
3. Pair multiplicity $\kappa_0 = a_0/(4\mu) > 1$

Under-dense zones in a conical $e^{\pm}$ jet/beam

Fluctuation wavelength $2\pi\lambda\!\!\!^{-}$ $a_0 \gg \mu \gg \sigma \gg 1$

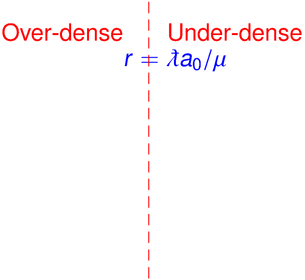

Under-dense zones in a conical $e^{\pm}$ jet/beam

Fluctuation wavelength $2\pi\lambda\!\!\!^{-}$ $\quad a_0 \gg \mu \gg \sigma \gg 1$

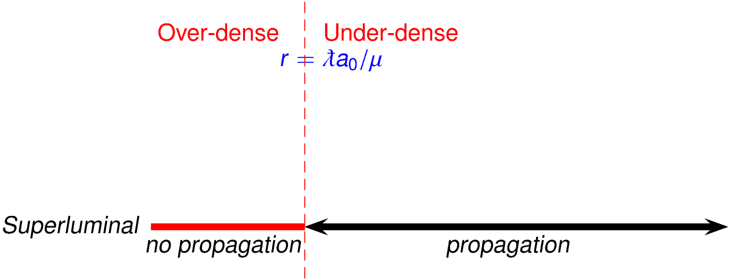

Under-dense zones in a conical $e^{\pm}$ jet/beam

Fluctuation wavelength $2\pi\lambda\!\!\!^{-}$ $a_0 \gg \mu \gg \sigma \gg 1$

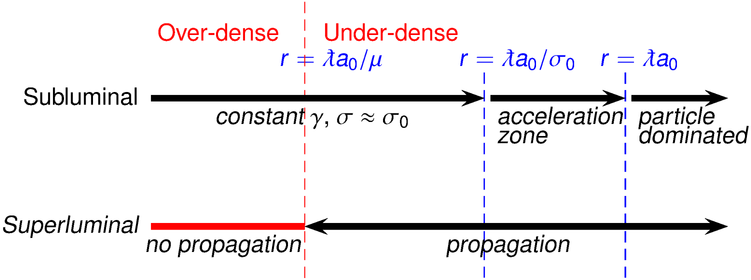

Under-dense zones in a conical $e^{\pm}$ jet/beam

Fluctuation wavelength $2\pi\lambda\!\!\!^{-}$ $\quad a_0 \gg \mu \gg \sigma \gg 1$

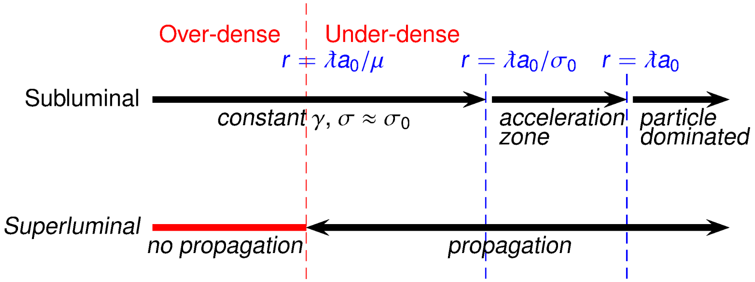

$\kappa_0 = 1$	4×10^{15}cm	10^{20}cm
$\kappa_0 = 10^3$	4×10^{18}cm	10^{22}cm

(Estimates for M87: $L = 10^{41}\,\mathrm{erg/s}$, $\Omega_s/4\pi = 0.0006$, $\lambda\!\!\!^{-} = r_g = 10^{15}\,\mathrm{cm}$)

Two-fluid simulations

Beyond MHD: simplest description that includes superluminal, electromagnetic modes is two-fluid $e^{\pm}$ Amano & Kirk ApJ (2013)

Initial conditions:

- Left half: circularly polarized, cold, static shear
- Supersonic: $\Gamma > \sigma^{1/2}$
- Under dense: $\lambda \lesssim c/\omega_{\rm p}$
- Search for quasi-stationary precursor

Precursor for $\Gamma_u = 100$, $\sigma = 25$

Snapshot at $\omega_{p0} t = 1000$

$\omega = 1.2\omega_{p0}$, $\omega = 2.5\omega_{p0}$, $\omega = 3.8\omega_{p0}$

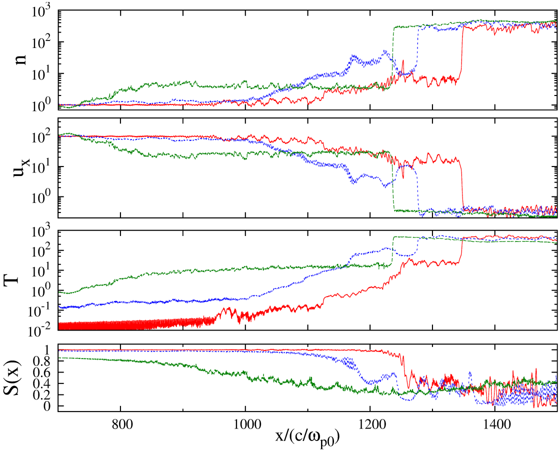

Steady state for $\Gamma_u = 100$, $\sigma = 25$, $\omega = 1.2\,\omega_{p0}$

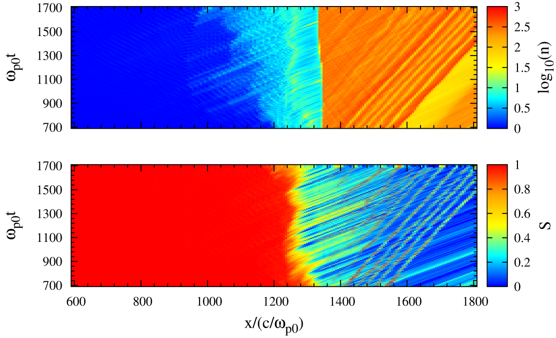

Steady state for $\Gamma_u = 100$, $\sigma = 25$, $\omega = 1.2\,\omega_{p0}$

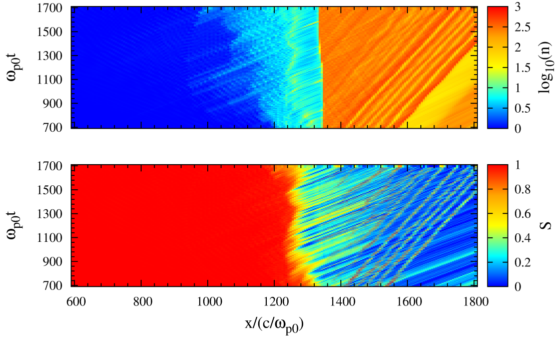

Stationary precursor for $\omega \gtrsim \omega_{p0} \iff R \gtrsim 1$

Test-particle trajectories

Particles followed to upstream or downstream boundary

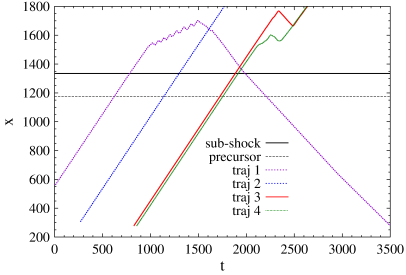

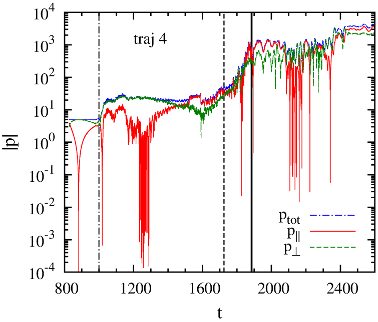

Electrons energized in precursor, reflected downstream.

Test-particle trajectories

Spectra on exiting

(local fluid frame)

Reflection probability $\approx$ 12%

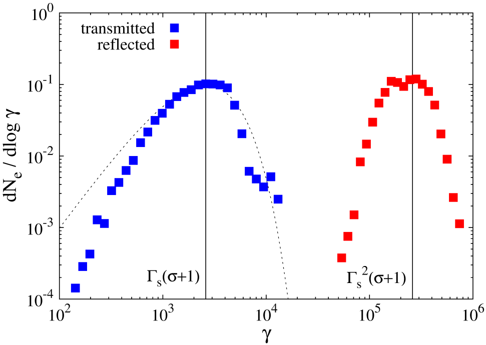

Monte-Carlo simulations of Fermi-I acceleration

- Shear wave (stripes) in upstream plasma
- Zero average field in downstream

Monte-Carlo simulations of Fermi-I acceleration

- Shear wave (stripes) in upstream plasma
- Zero average field in downstream
- Scattering length $\gg$ wavelength of (upstream) stripes

Monte-Carlo simulations of Fermi-I acceleration

- Shear wave (stripes) in upstream plasma
- Zero average field in downstream
- Scattering length $\gg$ wavelength of (upstream) stripes
- Two regimes:
  - Regime I: $r_{\mathrm{g}} \gg \lambda$ (injection by SL waves)
  - Regime II: $r_{\mathrm{g}} \ll \lambda$ (driven reconnection?)

Monte-Carlo simulations of Fermi-I acceleration

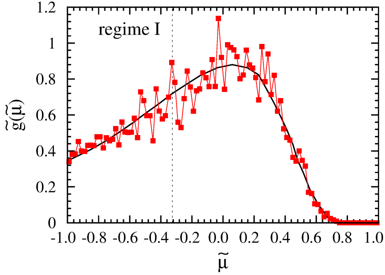

Black: asymptotic distribution for parallel shock

$s = 2.2$

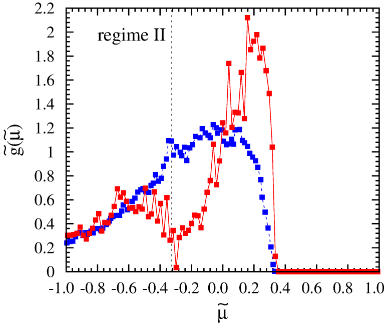

Blue: "Regular deflection" upstream, Achterberg et al (2001)

$s = 2.6$

Conclusions, outlook

Conclusions, outlook

- Energy stored in magnetic fluctuations dissipates at low density via reflected superluminal waves in a shock precursor.

Conclusions, outlook

- Energy stored in magnetic fluctuations dissipates at low density via reflected superluminal waves in a shock precursor.
- The precursor accelerates and reflects particles, injecting them into a Fermi-I mechanism with $\gamma \approx \gamma_{\max} = \sigma\Gamma$.

Conclusions, outlook

- Energy stored in magnetic fluctuations dissipates at low density via reflected superluminal waves in a shock precursor.
- The precursor accelerates and reflects particles, injecting them into a Fermi-I mechanism with $\gamma \approx \gamma_{\rm max} = \sigma\Gamma$.
- Subsequent acceleration produces the same power-law spectrum as a parallel, relativistic shock.

Conclusions, outlook

- Energy stored in magnetic fluctuations dissipates at low density via reflected superluminal waves in a shock precursor.
- The precursor accelerates and reflects particles, injecting them into a Fermi-I mechanism with $\gamma \approx \gamma_{\rm max} = \sigma\Gamma$.
- Subsequent acceleration produces the same power-law spectrum as a parallel, relativistic shock.
- 2D/3D: Effects of non-specular reflection? (Analogue of shock corrugation in MHD regime Lemoine et al (2016))